A NEW METHOD TO CALCULATE BENDING DEFORMATION OF INVOLUTE HELICAL GEAR

Wei SUN[1], Tao CHEN[2], Xu ZHANG[3]

The traditional method to calculate bending displacement of helical tooth is generally based on simplified tooth profile. Besides, the unbalance loading is not taken into account. To overcome this disadvantage, a new method to calculate bending deformation of helical tooth is introduced. First, gear section is divided into several copies along tooth width and each section's moment of inertia is calculated. Second, the unbalance loading of helical gear is calculated and distributed. Based on these work, a general formula for bending displacement of involutes helical gear is presented. Last, accuracy of this study is proved by an example.

Keywords: Tooth profile section; Moment of inertia; Load distribution; Bending deformation; Involutes helical gear.

1. Introduction

Helical gears are important transmission parts. Their bending deformation have always been one of the research focuses, and many scholars have done lots of work on it. The initial study is concerned on stress and deformation of gears [1, 3]. With further researches, vibration caused by meshing gears began to be the hot topic: Cai takes the spacing error and the shaft run-out into account, and establishes a nonlinear tooth model [4]. For mesh stiffness varies with rectangular waveforms, Jian and Parker, deduced simple design formulas to control the instability regions by adjusting the contact ratios and mesh phasing [5].

Generally, researches on bending deformation of loaded tooth mainly include analytical method, Finite Element Method (FEM) and experimental method [6, 7]. Typical experimental method is photoelasticity and laser speckle interferometry; results of the latter are compared to three analytical results in [8]. The reliable analytical methods are the energy method (also known as material mechanics method), which was raised by Weber [9], and the complex variable function method, which was developed by Aida and Terauchi [10, 12]. Traditional material mechanics method adopts the view of Lewis which regards tooth as an elastic

[1] Prof. and a Ph.D. candidate supervisor in School of Mechanical and Engineering, Dalian University of Technology, China
[2] Corresponding author. Ph.D. in School of Mechanical and Engineering, Dalian University of Technology, China. e-mail address: ct810719@163.com
[3] Post doctor in School of Mechanical and Engineering, Dalian University of Technology, China.

cantilever. On this basis, Ishikawa have deduced his algorithm and demonstrated that integrated elastic deformation of loaded tooth consist of tooth contact deformation, bending\shear\compression deformation of cantilever, and additional deformation of matrix [13, 14].

There are mainly two shortcomings of analytical solutions based on the traditional method. First, a simplified tooth profile is used and reduces the accuracy of results. Second, average tooth stiffness is used to calculate deformation of helical tooth and the unbalance loading along tooth width is not considered. In the case that the required precision is not rigorous, the simplified tooth profile and the average tooth stiffness can reluctantly meet the engineering requirements. But with the trends of high efficiency, high power and high reliability, the traditional analytic method has some limitations when applied on gear modification, dynamic noise suppression, etc.

However, researches on this topic and papers about this issue are relatively few. With the development of finite element technology and emulation technique, such calculations can be solved numerically [15, 18]. Thus, the analytical solution for the bending deformation of loaded tooth is rarely reported recently. But in most cases, the pre-processing and computing is very time-consuming, and it is hard to find a suitable analytical solution for comparison. So, a high-precision analytical solution on bending deformation of loaded tooth is still of great significant.

This paper analyzes the problem that exists in the conventional method of calculating the tooth bending deformation. The gear section is divided into numbers of copies and the two most important factors which affect tooth bending deformation are considered: variable moment of inertia caused by changing tooth profile and variable distributed load caused by changing length of contact line. In addition, the unbalance loading of helical gear is taken into account. We hope to derive the general bending deformation formula of involutes helical gear on the basis of material mechanics method. At the same time, an example is used to prove the accuracy of this method.

2 Elastic bending deformation of involutes helical gears

When gear tooth is in working conditions, the varied thickness leads to a change in stiffness. In addition, the alternate number of teeth leads to a change in load distribution. Focusing on the two points, a new method to calculate bending deformation of helical gear is deduced by the cross-section method. But first of all, the inertia moment of the cross-section and the distributed load along contact line are required.

2.1 Deformation of cross section

The gear tooth is divided into n copies along its spiral direction (the helix angle direction) as shown in Fig. 1. All sections are equal and tooth thickness varies from tooth root to tooth tip. Since moment of inertia is a geometric parameter, bending resistance of this irregular geometry is not exactly the same when the meshing radius varies. In order to quantify the bending deformation, any section is selected and orders that the original point of the coordinate system locates at its pitch circle.

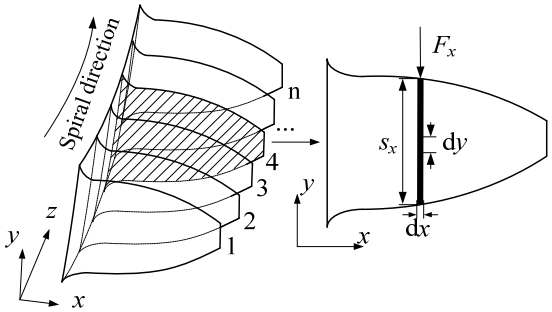

Fig. 1. Cross-sectional model of tooth cantilever

Bending deformation of a loaded cantilever can be easy obtained by the deflection curve equation, [19]. Ssuch geometry of unit width (right of Fig. 1) can be regarded as a cantilever model and the following equation is used to calculate the bending deformation along x-axis:

$$u = \iint \left(\frac{M_x}{EI_x} \mathrm{d}\, x \right) \mathrm{d}\, x + \mathrm{C}\, x + \mathrm{D} \tag{1}$$

where, C and D are integration constants; EI_x is the bending stiffness of this cantilever. M_x is the bending moment in the selected section. When the meshing radius is r_x, it can be written:

$$\begin{cases} M_x = -F_x(l - x) \\ l = r_x - r_{s_F} \end{cases} \tag{2}$$

where, r_{sF} is the radius of dangerous cross sections s_F [14]. One takes an infinitesimal unit along the direction of tooth thickness as shown in the right of Fig. 1. The moment of inertia is as follows:

$$I_x = \int_L y^{\,2} \mathrm{d}\, L_x$$

where, $\mathrm{d}\, L_x = \mathrm{d}\, y$

Thus:
$$I_x = \int_L y^{\,2} \mathrm{d}\, L_x = \int_{-s_x/2}^{s_x/2} y_x^{\,2} \mathrm{d}\, y = \frac{1}{12} s_x^{\,3} \tag{3}$$

s_x is the tooth thickness of meshing radius r_x , and according to the meshing gear principle, one can write:

$$s_x = s\frac{r_x}{r} - 2r_x(inv\alpha_x - inv\alpha_t) \tag{4}$$

where, α_t is transverse pressure angle of the pitch cercle. Comparing to the gear tooth, stiffness of the gear matrix is much greater, deformation of the dangerous cross sections u can be regarded as zero, and so does its angle of rotation θ. On this bases, we define the boundary conditions as follows:

$$\begin{cases} u\Big|_{r_x=r_{sF}} = 0 \\ u'\Big|_{r_x=r_{sF}} = \theta_{sF} = 0 \end{cases} \tag{5}$$

Hence, we can work out the integral constants: C=D=0. So, deflection curve equation of this tooth section can be expressed as:

$$u_x = \frac{12}{\mathrm{E}}\int\left(\int\frac{F_x(l-x)}{s_x^3}\mathrm{d}x\right)\mathrm{d}x \qquad x\in[r_{s_F}, r_a] \tag{6}$$

where, r_a is the radius of tooth tip and E is the Young modulus. By using Eq. (6), the deformation along the x-axis can be solved point by point. But before this, there is still another problem to take into account: the tooth load and its distribution along contact line.

2.2 Load distribution along the contact line

Besides the bending stiffness, another key reason related to tooth bending deformation is distributed load along contact line. Profile of a helical tooth is showed in Fig. 2; β_b is the base spiral angle and KK is the instantaneous meshing line. The plane of action w is rolling around the base cylinder.

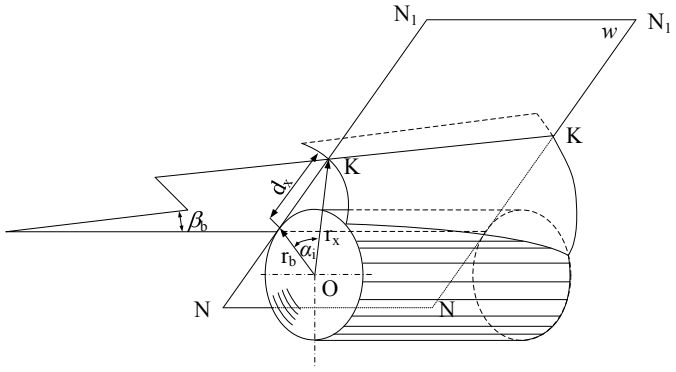

Fig. 2. Profile of helical tooth

Suppose that meshing status of the starting moment is double tooth meshing. r_x is the radius of meshing point K. When point K is moving along meshing line NN_1 the moved distance can be measured as follows:

$$d_x = \sqrt{r_x^2 - r_b^2} \tag{7}$$

For obtaining the distribution of tooth load, the engagement status and the length of contact line L_x are acquired. A complete meshing cycle is shown in Fig. 3, where, t_m is the time that gear rotated a distance of base circle pitch p_{bt}.

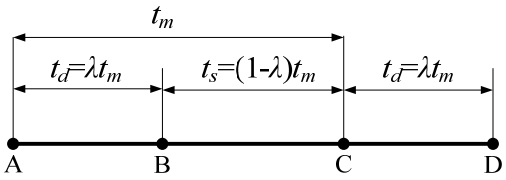

Fig. 3. Cycle of meshing tooth

It is easy to determine that:

$$\begin{cases} t_m = \dfrac{60}{n_0 z} \\ P_{bt} = m_t \pi \cos \alpha_t \\ \lambda = \varepsilon_\alpha - 1 \end{cases} \tag{8}$$

where, n_0 is the rotating speed of gear, z is the number of teeth, ε_α is the face contact ratio. So, the threshold between single tooth meshing and double tooth meshing can be established: when $0<t<(\varepsilon_\alpha\text{-}1)t_m$ or $t_m<t<\varepsilon_\alpha t_m$, status of meshing is double tooth engagement, and when $(\varepsilon_\alpha\text{-}1)\ t_m < t < t_m$, status of meshing is single tooth engagement.

Projection of tooth profile on the acting plane w is shown in Fig. 4. Symbols b and AE represent tooth width and mesh width, respectively. Solid line and dotted line represent two meshing moments separately [20]. Distribution of contact line on the tooth profile is decided by the transverse contact ratioε_α, face contact ratio ε_β and base spiral angle β_b. Different combinations of these three factors decide the changing velocity and distributed load along the contact line. Thus, the rule for load distribution is established: take the proportion of instantaneous contact line length in average contact line length as the reference of load distribution.

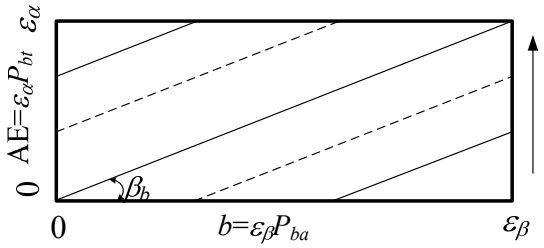

Fig. 4. Contact line of helical tooth

The average length of contact line can be obtained according to Eq. (9) [21, 22].

$$\begin{cases} L = \dfrac{\varepsilon_\alpha b}{\cos\beta_b} \\ \beta_b = \text{atan}(\tan\beta \times \cos\alpha_t) \end{cases} \tag{9}$$

The instantaneous length of contact line L_x can be calculated according to the geometric relationship in Fig. 4:

1) When $0<t<(\varepsilon_\alpha\text{-}1)t_m$, the meshing status is double tooth engagement and length of contact line is:

$$L_x = \frac{\left(\sqrt{r_x^{\,2} - r_{S_F}^{\,2}}\right)\varepsilon_\alpha}{\sin\beta_b} \tag{10}$$

2) When $(\varepsilon_\alpha\text{-}1)t_m<t<t_m$, the meshing status is single tooth engagement. There are three cases: If the contact point has not reached the tooth tip, Eq. (10) is still available. If the contact point has already reached the tooth tip, the length of contact line will tend to stabilize and the average length L can measure the contact line length in this region. In the late period of single tooth engagement, the contact line length will shorten according to Eq. (11).

$$L_x = \frac{\left(\sqrt{r_a^{\,2} - r_x^{\,2}}\right)\varepsilon_\alpha}{\sin\beta_b} \tag{11}$$

3) When $t_m<t<\varepsilon_\alpha t_m$, the meshing status is double tooth engagement again, the length of contact line continues to shrink according to Eq. (11) and withdraws from meshing gradually.

Then, the tangential load F_t can be distributed based on the length of instantaneous contact line as follows:

$$F_{tx} = \frac{L_x F_t}{L} \tag{12}$$

F_{tx} is the total load acting on the selected contact line. In addition, the unbalance loading along contact line must be considered. Supposing that f_2 is

greater than f_1 and distance between f_x and f_1 is Δl. If one unfolds the contact line of tooth profile, a straight line is obtained. We can define line load f_x according to a trapezoid. There is:

$$f_x = f_1 + \frac{\Delta l(f_2 - f_1)}{L_x} \tag{13}$$

The line load f_1 and f_2 can be structured by the following equation.

$$\begin{cases} \dfrac{(f_1 + f_2)}{2} = F_{tx} \\ f_2 - f_1 = k_f z_\beta \beta F_{tx} \\ z_\beta = \sqrt{\cos\beta} \end{cases} \tag{14}$$

where, β is the helical angle, z_β is the helical angle factor and $k_f \in$ (1.05~1.2). Then, the line load f_x can be solved according to Eq. (14):

$$f_x = F_{tx}\left(1 - \frac{k_f \beta\sqrt{\cos\beta}(L_x - 2\Delta l)}{2L_x}\right) \tag{15}$$

When the force F_t is given, the unbalanced load on the contact line is related to the length of the contact line, helical angle, and helical angle factor. The distance Δl is decided by the position of meshing point.

2.3 Elastic bending deformation of helical tooth

After calculating the cross section moment of inertia and quantifying the distributed load along contact line, the tooth displacement of the selected section can be deduced. And then, we can further deduce the deformation formula of a certain every tooth section. Aditional displacement is calculated here for the reason that it is closely related to aditional modification and other engineering parameters.

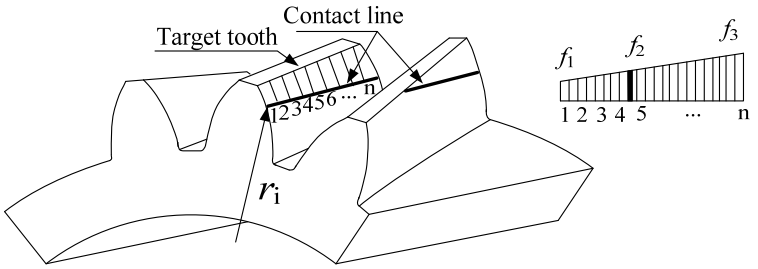

Fig. 5. Mesh track of helical tooth

Consider the middle tooth as object which is shown in Fig. 5. The load position of each section is different and load changes continuously due to the

unbalance loading of helical gear. Consider section *No*. 5 for example (k=5); load radius of this section is as follows, where n is the number of sections.

$$r_i' = r_i - \frac{kb}{n-1}\tan\beta \qquad k = 5 \tag{16}$$

The equation for displacement of section *No*. 5 is calculated according to Eq. (6) and its aditional deformation is calculated as:

$$\begin{cases} u_x = \dfrac{12}{\mathrm{E}}\int\left(\int \dfrac{f_x(l-x)}{s^3{}_x}dx\right)dx & x = r_i' \\ u_a = u_{r_i} + (r_a - r_i')\tan\theta_{r_i} \approx u_{r_i} + (r_a - r_i')\theta_{\max} \end{cases} \tag{17}$$

Radius r_i in Eq. (17) will be substituted by (r_i+Δr) when gears rotate with a small angle $\Delta\theta$. Transformation between $\Delta\theta$ and Δr can be achieved from transverse profile as follows:

$$\Delta\theta = \arccos\frac{r_b}{r_i + \Delta_r} - \arccos\frac{r_b}{r_i} \tag{18}$$

Displacement along contact line can be obtained by connecting series of discrete data. We can predict that this trend is nonlinear and varies with the meshing point.

3 Example and comparison

3.1 Example

Without loss of generality, one considers a pair of ordinary helical gear for example. The major parameters are listed in Table 1. The surface hardness is 680HB and addendum modification is needed. Therefore, aditional deformation is needed to be calculated according to this study. Only pinion is selected as the object.

Table 1

Parameters of gear tooth

Parameters	Value	Parameters	Value
Tooth number	z_1=21 z_2=86	Normal pressure angle	α_n=20°
Normal module	m_n=8mm	Tooth width	b=160mm
Face contact ratio	ε_β=1.105	aditional coefficient	h∗=1.0
Power	750KW	Helical angle	β=8°
Modification coefficient	x_1=0.47	x_2=0.51	

The tooth section is divided into several copies along the tooth width. By determining the load location and load magnitude, the aditional displacement is solved point by point using the method presented in this paper. The number of sections can be increased if a higher precision is needed. This model is calculated

using MATLAB because integral function as Eq. (17) cannot be solved by an analytical algorithm. Three meshing points r_x are selected in each engagement status separately. Results (partial and full engagement) are listed in Table 2 and Table 3 separately.

Table 2

Addendum deformation of partial engagement

/ 10^{-3}mm

r_i=88	n=11	n=12	n=13	n=14	n=15	n=16	n=17	n=18
	4.7258	5.6170	6.4782	7.3094	8.1105	8.8870	9.6340	10.352
	n=19	n=20	n=21					
	11.041	11.695	12.322					
r_i=90	n=14	n=15	n=16	n=17	n=18	n=19	n=20	n=21
	4.2619	5.1049	5.9179	6.7009	7.4537	8.1764	8.8745	9.5427
r_i=92	n=16	n=17	n=18	n=19	n=20	n=21		
	2.8952	3.7206	4.5155	5.2802	6.0148	6.7193		

Table 3

Addendum deformation of full engagement

/ 10^{-2}mm

r_i=90	n=1	n=2	n=3	n=4	n=5	n=6	n=7	n=8	n=9
	2.269	2.2851	2.3012	2.3173	2.3335	2.3497	2.3659	2.3821	2.3983
	n=10	n=11	n=12	n=13	n=14	n=15	n=16	n=17	n=18
	2.4145	2.4308	2.4471	2.4634	2.4797	2.4961	2.5124	2.5288	2.5452
	n=19	n=20	n=21						
	2.5616	2.5781	2.5945						
r_i=92	n=1	n=2	n=3	n=4	n=5	n=6	n=7	n=8	n=9
	2.2711	2.2872	2.3033	2.3195	2.3356	2.3518	2.368	2.3842	2.4005
	n=10	n=11	n=12	n=13	n=14	n=15	n=16	n=17	n=18
	2.4168	2.433	2.4493	2.4657	2.482	2.4983	2.5147	2.5311	2.5475
	n=19	n=20	n=21						
	2.564	2.5804	2.5969						
r_i=94	n=1	n=2	n=3	n=4	n=5	n=6	n=7	n=8	n=9
	2.2732	2.2893	2.3054	2.3216	2.3378	2.354	2.3702	2.3864	2.4027
	n=10	n=11	n=12	n=13	n=14	n=15	n=16	n=17	n=18
	2.419	2.4353	2.4516	2.4679	2.4842	2.5006	2.517	2.5334	2.5498
	n=19	n=20	n=21						
	2.5663	2.5828	2.5992						

3.2 Comparison of results

The same tooth pair is selected as in Tab. 1. Aditional bending displacement, are calculated separately using the method proposed here, the Ishikawa algorithm, and FEM for the purpose of verifying the correctness and

accuracy of the new method. The tooth cross section is considered as a combination of rectangle and trapeze in the Ishikawa algorithm, and the dangerous section is decided by the method of 30° tangent. Specific process refers to literature [13, 14].

The 3D FEM model was established and meshed before calculating as showed in Fig. 6. Nonlinear contact pairs are created, rotational freedom of driven gear is bounded, and rotating torque is applied to driving gear. The middle tooth is selected as object. Tangential deformation of aditional node is extracted as tooth addendum deformation. Inaccuracy will be existed spans from contact area to non-contact area along tooth width in state of partial engagement, but the error is tiny according to St-Venant principle [23].

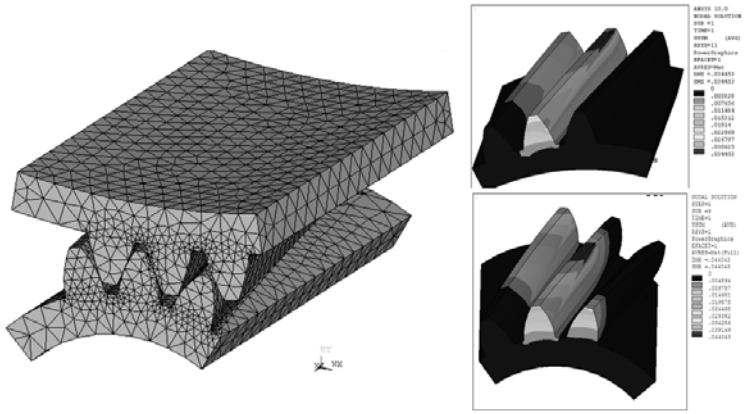

Fig. 6. Tooth finite element model and deformation plot

Both in the full engagement and partial engagement, results of the three methods are plotted in Figs. 7 and 8 separately, aditional displacement along tooth width shown in the graphs.

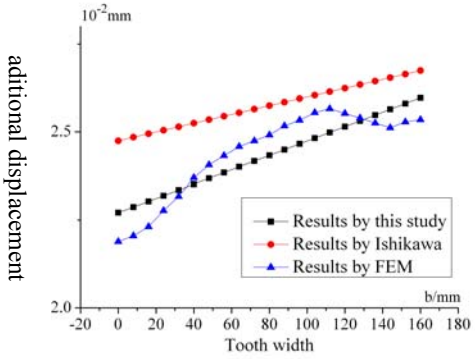

Fig. 7. Results of three methods in full engagement status

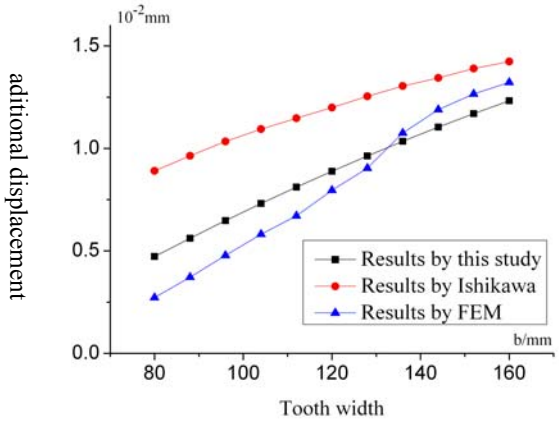

Fig. 8. Results of three methods in partial engagement status

Results of Fig. 7 and Fig. 8 indicate that: Bending deformation calculated by Ishikawa method is greater than results calculated by FEM and this study due to simplified tooth profile and average stiffness; At the same time, nonlinearity trend of FEM result is more obvious due to influences of node singularity, loading mode, and so on. Compared to Ishikawa method, results of FEM and this study are in good agreement. If the results of FEM are considered as baseline, the standard deviation of Ishikawa method and this study can be calculated according to data of Fig. 7 and Fig. 8. When in full engagement status:

$$\begin{cases} \delta_{F_{(T-I)}} = \sqrt{\sum_{i=1}^{n}(u_{T_i} - u_{I_i})^2} = 0.7051\times10^{-2} \\ \delta_{F_{(T-F)}} = \sqrt{\sum_{i=1}^{n}(u_{T_i} - u_{F_i})^2} = 0.25547\times10^{-2} \end{cases} \tag{20}$$

and when in partial engagement status:

$$\begin{cases} \delta_{P_{(T-I)}} = \sqrt{\sum_{i=1}^{n}(u_{T_i} - u_{I_i})^2} = 1.3858\times10^{-2} \\ \delta_{P_{(T-F)}} = \sqrt{\sum_{i=1}^{n}(u_{T_i} - u_{F_i})^2} = 0.4307\times10^{-2} \end{cases} \tag{21}$$

where: u_T- aditional displacement calculated by this study;

u_F—aditional displacement calculated by FEM;

u_I—aditional displacement calculated by Ishikawa method;

We can see that, when results of FEM are considered as baseline, standard deviation of this study' results is much smaller than the one calculated for Ishikawa method in both conditions. It is easy to draw a conclusion that accuracy of this study is better than traditional analytical solution.

In addition, compare to partial engagement, load on contact line is well-distributed in full engagement because of the long contact line and small unbalance loading. We can calculate the average gradient in both conditions. When in full engagement status:

$$\begin{cases} k_{F-I} = \dfrac{u_{\max} - u_{\min}}{L} = \dfrac{2.6745 - 2.4755}{160} = 1.2438 \times 10^{-3} \\ k_{F-T} = \dfrac{u_{\max} - u_{\min}}{L} = \dfrac{2.5969 - 2.2711}{160} = 2.2036 \times 10^{-3} \\ k_{F-E} = \dfrac{u_{\max} - u_{\min}}{L} = \dfrac{2.5661 - 2.1890}{160} = 2.3569 \times 10^{-2} \end{cases} \tag{22}$$

and when in partial engagement status:

$$\begin{cases} k_{P-I} = \dfrac{u_{\max} - u_{\min}}{L} = \dfrac{1.4242 - 0.8902}{80} = 6.675 \times 10^{-3} \\ k_{P-T} = \dfrac{u_{\max} - u_{\min}}{L} = \dfrac{1.2322 - 0.4726}{80} = 9.495 \times 10^{-3} \\ k_{P-E} = \dfrac{u_{\max} - u_{\min}}{L} = \dfrac{1.3222 - 0.2726}{80} = 13.1 \times 10^{-3} \end{cases} \tag{23}$$

where: k_T—Average gradient calculated by this study;

k_F—Average gradient calculated by FEM;

k_I—Average gradient calculated by Ishikawa method;

Average gradient in full engagement status smaller than in partial engagement status, respectively, in three under the three results. Thus, the curve in full engagement status changes mildler; by contrast, the curve in partial engagement status changes more abruptly.

4. Conclusions

A new method to calculate elastic bending deformation of helical tooth is introduced using cross sectional moment of inertia and distributed load. The moment of inertia in the real profile section is calculated; the unbalance loading is considered along the tooth profile and the tooth load is distributed at each meshing moment. Based on these studies, general formula of helical tooth elastic deformation is derived. In addition, aditional bending deformation with the method proposed in this study, Ishikawa algorithm, and FEM are calculated and compared. Standard deviation is used to verify the accuracy of this study. Here are the major conclusions of this paper:

(1) Continuously varied moment of inertia due to changing tooth thickness during engagement is the major reason for non-uniform tooth stiffness.
(2) Distribution and changing rate of contact line on the tooth profile are largely affected by transverse contact ratioε_α, face contact ratio ε_β and base spiral angle β_b.
(3) The unbalanced loading of helical tooth is related to the length of the contact line, helical angle and helical angle factor, and the unbalanced load lead to a faster load changes in the contact line.
(4) Curve changes milder due to the long contact line and small unbalance loading in full engagement status. The average gradient is notable small under this condition.
(5) The accuracy of this study is better than the traditional analytical solution, and it can provide valuable data for aditional modification.

Acknowledgements

Thanks must be given to Gear Research Institute of Taiyuan Heavy Industry Group, Taiyuan, Chain, for providing drawings and data for the authors to finish part of this research. This work has been also motivated by senior engineer of Ai'gui Guo in Taiyuan Heavy Industry Group for his useful comments and suggestions.

R E F E R E N C E S

[1]. *R V Band and R E Peterson*, "Load and Stress Cycle in Gear Teeth", Mechanical Engineering, **Vol. 51**, no. 9, 1929, pp. 653-662
[2]. *C W Mac Gregor*, "Deformation of a Long Helical Tooth", Mechanical Engineering, **Vol.157**. 1935
[3]. *T Tobe, M Kato and K Inone*, "Effects on the Inclination of the Root on the Deflection of Gear Teeth (In Japanese)", Trans Japan Soc. Mech. Engres, **Vol. 39,** 1973, pp. 3473-3480
[4]. *Y Cai*, "Simulation on the Rotational Vibration of Helical Gears in Consideration of the Tooth Separation Phenomenon (a new stiffness function of helical involute tooth pair)", Journal of Mechanical Design, ASME, **Vol. 117**, no. 3, 1995, pp. 460-469
[5]. *Lin Jian and R G. Parker*, "Mesh Stiffness Variation Instabilities in Two-stage Gear Systems", Journal of Vibration and Acoustics, ASME, **Vol. 124**, no. 1, 2002, pp. 68-76
[6]. *R W Cornell*, "Compliance and Stress Sensitivity of Spur Gear Teeth", Journal of Mechanical Design, ASME, **Vol. 103**, 1981, pp. 447-459
[7]. *R.W. Furrow, H.H. Mabie*, "The Measurement of Static Deflection in Spur Gear Teeth", Journal of Mechanisms, **Vol. 5**, no. 2, 1970, pp. 147-150
[8]. *Zong-De Fang and Xiao-Yu Jiang*, "Deformation of Loaded Tooth by Laser Speckle Interferometry", Journal of Mechanical Transmission, **Vol. 8**, no. 5, 1985, pp. 19-25

[9.] *C Weber*, "The Deformation of Loaded Gears and the Effect on Their Load-carrying capacity", Sponsored Research (Germany), British Scientific and Industrial Research., London, Report no. 3, 1949
[10]. *Y Teranchi and K Nagamura*, "On Tooth Teflection Calculation and Profile Modification of Spur Gear Tooth", In Proceedings of International Symposium on Gearing and power Transmission, Tokyo, Japan, 1981
[11]. *Y Teranchi*, *Nagamura and Kazuteru*, "Study on Deflection of Spur Gear Teeth (1st Report)", Bull JSME, **Vol. 184**, no. 23, 1980, pp. 1682-1688
[12]. *Y Teranchi*, *Nagamura and Kazuteru*, "Study on Deflection of Spur Gear Teeth (2st Report)", Bull JSME, **Vol. 188**, no. 24, 1980, pp. 447-452
[13]. *J.Ishikawa* "Deflection of Gear (in Japanese)", Trans Japan Soc. Mech. Engres, **Vol. 17**, 1951, pp.103-106
[14]. *Ru-Zeng Li and Qing-Hui Zhao* translated, Gear Strength Design Data, Mechanical Industry Press, Beijing, China, 1984
[15]. *Jesper Brauer*, "A General Element Model of Involute Gears", Finite Elements in Analysis and Design, **Vol. 40**, no. 13-14, 2004, pp. 1857-1872
[16]. *Ani Ural, Gerd Heber and Paul A Wawrzynek,* etc. "There-dimensional, Parallel, Finite Element Simulation of Fatigue Crack Growth in a Spiral Bevel Pinion Gear", Engineering Fracture Mechanics, **Vol. 72**, no. 8, 2005, pp. 1148-1170
[17]. *Chien-Hsing Li*, *Hong-Shun Chiou and Chinghua Hung*, etc. "Integration of Finite Element Analysis and Optimum Design on Gear Systems", Finite Elements in Analysis and Design. **Vol. 38**, no. 3, pp. 2002, 179-192
[18]. *Runfang Li*, Finite Element Analysis of Meshing Gear as a Coupled Thermo-elastic Contact Problem, Proc Inter Conf on Gears, Zhengzhou, China, 1988
[19]. *Hong-Wen Liu*, Mechanics of Materials, Higher Education Press, Beijing, China, 1992
[20]. *Zhimin Fan and A. Guanghui Zhang*, "Analysis on Meshing Characters of double involute gear with ladder shape teeth," Chinese Journal of Mechanical Engineering, **Vol. 38**, no. 9, 2002, pp. 73-76
[21]. *Shouwei Feng, Shenling Zhang and Tao Zhang*, "Contact Line Length and Contact Ratio Coefficient of Cylindrical Gears", Journal of Chang'an University, **Vol. 24**, no. 2, 2004, pp. 101-103
[22]. *K Hayashi*, "Load Distribution on the Contact Line of Helical Gear Teeth", Bull. ASME, **Vol. 233**, no. 27, 1984, pp. 2336-2343
[23]. *Jia Long*, Theory of Elastic Mechanics, Tongji University Press. Shanghai, China, 1996